Polariton-polariton interaction potentials determination by pump-probe degenerate scattering in a multiple microcavity

Thimotée Lecomte, David Taj, Aristide Lemaitre, Jacqueline Bloch, Claude Delalande, Jérôme Tignon, Philippe Roussignol

Polariton-polariton interaction potentials determination by pump-probe degenerate scattering in a multiple microcavity

Timothée Lecomte,[1, a] David Taj,[1, b] Aristide Lemaitre,[2] Jacqueline Bloch,[2]
Claude Delalande,[1] Jerome Tignon,[1] and Philippe Roussignol[1]

[1] *Laboratoire Pierre Aigrain, École Normale Supérieure, CNRS (UMR 8551), Université P. et M. Curie, Université D. Diderot, 75231 Paris Cedex 05, France.*
[2] *LPN/CNRS, Route de Nozay, F-91460 Marcoussis, France.*

(Dated: April 12, 2014)

We study the polarisation-dependent polariton-polariton interaction through its effect on a parametric scattering process in a microcavity (MC). The ratio of the anti-circular interaction strength V_2 over its co-circular counterpart V_1 is involved in defining the regime in which many nonlinear processes arise in MCs, such as parametric conversion or condensation. We measure the ratio V_2/V_1 using a stimulated energy-degenerate parametric scattering process in a multiple MC. The sample is pumped at normal incidence, probed with a non-zero angle, and the phase-matched idler is observed at the opposite angle. The idler behaviour, both in power and polarisation, is compared to a hamiltonian interaction model that takes into account the two polarisation-dependent parametric scattering channels characterized by V_1 and V_2. The proposed method to measure the ratio V_2/V_1 is convenient and precise. The flexibility of the triple MC allows to observe the process and measure this ratio over a large range of detunings, where we find it to be highly dependent on the detuning. These measurements complement the previous study of Vladimirova *et al.* [Phys. Rev. B 82, 075301 (2010)] with an original approach and for detunings that were unexplored up to now.

PACS numbers: 68.65.-k, 73.21.-b, 78.67.Pt, 71.36.+c

I. INTRODUCTION

Semiconductor microcavities (MCs) are a model system where numerous exotic optical effects can be observed: parametric amplification[1] and oscillation[2,3], polariton condensation[4], vortices inside condensates[5], polariton superfluidity[6], analogues of magnetic monopoles[7], etc. These phenomena involve interactions between polaritons, mixed states of confined photons and quantum well (QW) excitons. Those quasi-particles inherit interesting properties from each of their two strongly-coupled components. Their excitonic part brings Coulombian interaction, and the photonic part brings cavity amplification and steep dispersion. They have two allowed spin states, and in turn the interaction effects are strongly spin-dependent. In particular, we distinguish the interaction potential V_1 between polaritons of the same circular polarisation, and the potential V_2 between polaritons of opposite circular polarisation. The behaviours of the non-linear phenomena heavily depend[8,9] on the sign of V_1 and V_2 and on the ratio V_2/V_1. For example, a gas of polaritons in a planar cavity at zero temperature will either condensate in the real-space (i.e. collapse spatially) or in the reciprocal space depending[9] on V_1 and V_2. Similarly, the existence of a polarization bistability[10,11] and the feasibility of exciton polariton spin-switching[12] depend on the sign and value of V_2/V_1. The value of V_2/V_1 also determines directly how the gain of a parametric amplifier depends on the polarisation configuration, as illustrated in this work.

Parametric amplification was first observed in a single MC[1] in a co-circular configuration, whereas no gain was visible in the anti-circular setup. This indicated that the potential V_2 was noticeably smaller than V_1, as other studies confirmed[13,14]. Direct experimental studies of the relative value of V_2 followed. Based on the spin-resolved temporal evolution of the polariton populations[15,16], it was found that V_2 was approximately ten times smaller than V_1 and of the opposite sign. The latter was confirmed by the rotation of the linear polarisation in spontaneously-formed continuous-wave optical parametric oscillation in a MC[11,17]. Studying the polarisation degree of MC luminescence[18], the value of $V_1 + V_2$ was evaluated. The measure of the blueshift and of the broadening of the polariton lines in a MC with two coupled QWs under an electric field was proposed[19] as a way to measure V_1 and V_2. Nevertheless the dependence of the values of these potentials as a function of energy has kept being neglected when interpreting MC experiments. Meanwhile, various theoretical studies focused on V_2. In Ref. 20 the spin-dependent interaction between Wannier excitons in a crystal is estimated. In Ref. 21 a model of the spin-dependant exciton-exciton elastic scattering is proposed. In Ref. 22, the consequences of the spin-dependent interactions on the dark excitons and on the polariton condensation are studied. In Refs. 23–25 the interaction mechanisms are studied using scattering matrices made of polarisation states. The recent work of Ref. 9 focused on measuring experimentally V_2/V_1 through the spin-resolved and energy-resolved nonlinear transmission of a MC. The ratio is found to strongly depend on the energy detuning and is compared to a theoretical model of the underlying interaction mechanisms. Since the ratio V_2/V_1 has a major effect on the nature

of processes found in MCs, we aim at using an original approach to confirm that V_2/V_1 is not constant and to explore further the effect of the detuning.

Here, we propose to use a multiple MC as a tool to investigate the properties of the potentials V_2 and V_1. A multiple MC is a layered structure designed to produce a rich set of resonant parametric processes between polaritons. Although parametric amplification and oscillation have been observed in single planar MCs[1,26,27], those processes are limited to "magic-angle" configurations where the pump has to excite the sample at a very precise angle so that energy and momentum are conserved in the nonlinear process. This severely limits the range of accessible configurations. In a multiple planar MC, several cavities are stacked on top of each other and coupled by their intermediate mirrors. Appropriate coupling results in several delocalized modes of polaritons and a fan of accessible branches, enabling interbranch parametric processes to occur. The set of four-wave mixing configurations that conserve both energy and wave-vectors is consequently much richer. For example, parametric amplification and oscillation have been observed in a triple MC in an angle-degenerate configuration[3,28,29].

In the present paper, we show that parametric scattering in a multiple MC provides a direct and precise measure of V_2/V_1 over a large range of unexplored detunings, thus providing a reference to predict and interpret spin-dependent phenomena in MC[8]. The flexibility of the multiple MC allows us to study the potentials V_2 and V_1 over a very wide range of detunings compared to previous works. We specifically focus on a pump-probe parametric scattering that is degenerate in energy so that we can precisely describe the energy dependence of the ratio V_2/V_1. In this geometry, the sample is pumped at normal incidence and probed at the same energy in the lower polariton branch with a non-zero angle. The parametric scattering produces an idler at the opposite angle, phase-matched with the probe. We first verify that the process is unambiguously of parametric origin by studying the power behaviour of the ider, compared to an hamiltonian model of the parametric interaction between polaritons. Then we study the behaviour of the pump-probe process in relation to polarisation, compared to the hamiltonian model augmented to take into account the two polarisation-dependent scattering channels described by the potentials V_1 and V_2. We then deduce the value of the ratio of the interaction potentials V_2/V_1. The energy-degenerate configuration makes the interpretation of our results straightforward and very slightly dependent on fit parameters. We show that the value of V_2/V_1 strongly depends on the laser-exciton detuning.

II. PARAMETRIC DIFFUSION IN RESONANT EXCITATION

The sample used for this study is made of three coupled cavities grown using molecular beam epitaxy (Fig. 1). The three cavities are made of a total of four distributed Bragg reflectors (DBRs) with 13, 13, 13 and 25 $Al_{0.05}Ga_{0.95}As$ and AlAs pairs. The structure is meant to be studied in reflection, so it was designed with a thick back mirror. The two outer cavities both contain three $In_{0.07}Ga_{0.93}As$ QWs, with a 1s excitonic transition at 1.4754 eV. The inner cavity is empty. Although two cavities are enough to produce the necessary modes for a triply-resonant energy-degenerate scattering process, here a third cavity is interleaved to serve as an adjusting knob for the cavity coupling. The outer cavities are wedged in the same direction, so that they are always resonant and the position of the cavity modes can be adjusted by studying an appropriate position on the surface of the sample. The resonance of the inner cavity is placed at an energy high above the two others, and above the excitonic transition, so that the inner cavity just behaves as a mirror for the two outer cavities. It is wedged perpendicularly to the outer cavity wedges, providing an effective mirror of adjustable reflectivity, which allows to vary the optical coupling between the two outer cavities. The sample is cooled down to 5 K in a cold-finger, liquid-helium cryostat.

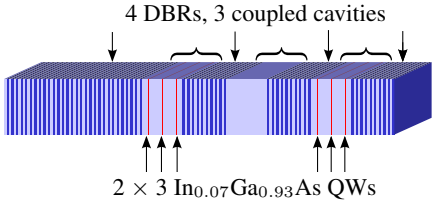

FIG. 1. (Color online) Structure of the asymmetric triple MC.

Consequently, the structure is made of three optical modes and two excitons (one set for each outer cavity), which gives five polariton branches. The Fig. 2 shows a typical dispersion obtained by nonresonant photoluminescence, where four polariton branches are visible. This dispersion was obtained in the case where the two outer cavities and the excitons are degenerate. The fifth polariton branch is essentially composed of the inner cavity mode, and lies at a higher energy. The four visible polariton modes are mixed states of excitons and photons delocalized in the two outer cavities. The Rabi splitting, which describes the coupling between excitons and photons and corresponds to the distance between the two lower polariton and their higher counterparts, is 6 meV. The two degenerate outer cavities gives delocalized modes separated by 1 meV, as can be seen by the distance between the first two lower polariton branches.

The sample is excited in a pump-probe configuration as shown if Fig. 3. The excitation is realized with a tunable cw Ti:Sapphire laser. The laser beam is splitted in two beams both focused on the sample surface. The pump spot diameter is 50 μm. The probe spot is made appropriately smaller. Attention is paid to proper beam superposition, and correct incidence angles. The

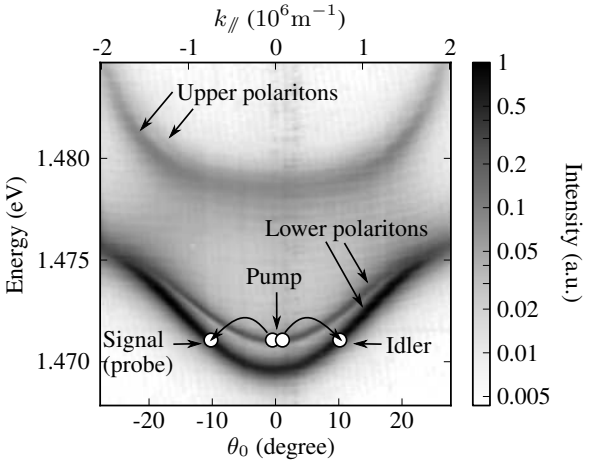

FIG. 2. Dispersion of the polaritonic modes obtained by photoluminescence under nonresonant excitation. Four polariton branches are visible. The energy-degenerate scattering process at stakes is schematically represented on the dispersion.

beams that are produced or reflected by the sample are observed with two CCD cameras: one is focused on the near-field and used to control the spots sizes and their superposition on the sample, and the second is focused on the far-field (i.e. the back focal plane of the excitation lens), behind a 50 cm spectrometer, to measure energy dispersions (Fig. 2) and resonant emission diagrams in the Fourier plane (Fig. 4).

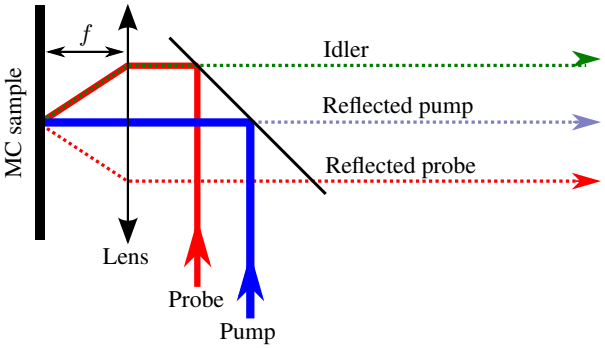

FIG. 3. (Color online) Excitation and visualisation setup for the reflective pump-probe experiment.

The pump and the probe beams are degenerate in energy. While the pump beam excites the second lower polariton branch at normal incidence, the probe beam excites the first lower polariton branch with a non-zero angle (Fig. 2). When these conditions are met, and when the pump and probe energy is chosen close enough to the exciton, an additional beam is observed coming from the sample, as shown on Fig. 4. It has the same energy as the two input beams and its wave-vector is the symmetric of the probe wave-vector with respect to the pump wave-vector. This beam is identified as the *idler* produced by the parametric scattering of pump polaritons stimulated by the presence of probe polaritons.

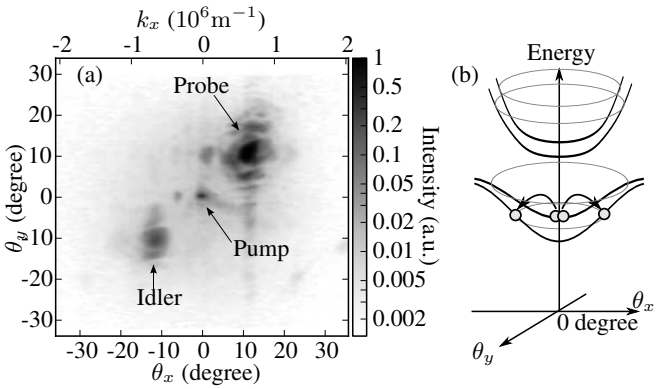

FIG. 4. (a) Image of the parametric scattering process in the Fourier plane of the excitation lens. The polarisations of the pump and the probe are perpendicular. The idler has the same polarisation as the probe. A polariser blocks most of the reflected pump. (b) Schematic view of the energy dispersion of the polaritonic modes against energy and angle and of the parametric process.

In the Fourier plane, the conservation of momentum imposes that the idler is always the symmetric of the probe with respect to the pump. This is verified by moving the probe beam on a ring as shown on Fig. 5. It is also possible to tilt the pump slightly, as long as the pump and the idler remain close to the modes of the structure. We then observe that the idler follows the tilt of the pump by staying the symmetric of the probe.

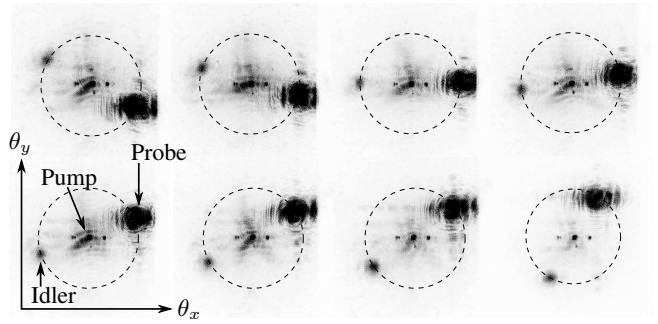

FIG. 5. Images of the parametric scattering process in the Fourier plane, in conditions similar to those of Fig. 4. The probe is moved over a ring centred on the pump, while the spots of the probe and the pump remain superposed on the surface of the sample. The idler follows the probe position in the Fourier plane, showing the momentum conservation.

III. MODEL OF INTERACTING POLARITONS

We will compare the experimental results to a model describing the polaritonic excitations in second quantization with the hamiltonian $H = H_0 + H_{int}$ obtained by truncating the coupled excitons-photon hamiltonian to

the second order in exciton density, and developing it in the basis of polaritons[21,30]. H_0 gives the linear behaviour of the polaritons and H_{int} describes the interaction between polaritons, that comes from their excitonic part:

$$H_0 = \sum_{\sigma=\pm} \hbar\omega \left(p^\dagger_{p\sigma} p_{p\sigma} + p^\dagger_{s\sigma} p_{s\sigma} + p^\dagger_{i\sigma} p_{i\sigma} \right) \tag{1}$$

$$\begin{aligned} H_{int} = \sum_{\sigma=\pm} \Big(& V_1(q=0) p^\dagger_{p\sigma} p^\dagger_{p\sigma} p_{p\sigma} p_{p\sigma} \\ & + V_2(q=0) p^\dagger_{p\sigma} p^\dagger_{p-\sigma} p_{p\sigma} p_{p-\sigma} \\ & + V_1(q=\kappa)(p^\dagger_{p\sigma} p^\dagger_{p\sigma} p_{s\sigma} p_{i\sigma} + h.c.) \\ & + V_2(q=\kappa)(p^\dagger_{p\sigma} p^\dagger_{p-\sigma} p_{s\sigma} p_{i-\sigma} + h.c.) \Big) \end{aligned} \tag{2}$$

$p_{p/s/i,\sigma}$ are the annihilation operators for the pump, probe (or signal) and idler polaritons respectively, with circular polarisation $\sigma = \pm$. In our degenerate configuration, $\hbar\omega = \hbar\omega_p = \hbar\omega_s = \hbar\omega_i$ is the single particle energy of the modes. $V_{1/2}$ are the interaction potentials for the co-circular and anti-circular polarisation scattering channels, respectively. The first two terms in $H_{\rm int}$ correspond to the Kerr effect (or *blueshift*) caused by the interaction of pump polaritons between each other. The last two terms correspond to the parametric scattering of two pump polaritons into a signal polariton and an idler polariton, respectively conserving or inverting the circular polarisation. $q = \kappa$ is the distance in momentum between the pump and the signal. H_{int} contains only the four interaction channels that are of importance in our configuration. We have neglected the terms for the cross Kerr effect ($p^\dagger_{p\sigma} p^\dagger_{p\sigma} p_{s\sigma} p_{s\sigma}$ and $p^\dagger_{p\sigma} p^\dagger_{p\sigma} p_{i\sigma} p_{i\sigma}$) and all other terms where the signal and the idler operators appear at a superior order.

This hamiltonian gives a set of coupled differential equations for the mean fields which boils down to the linear system $Mv = S$, for the time-independent complex-valued vector $v = (p_{s+}, p^*_{i+}, p_{s-}, p^*_{i-})$, where M is:

$$M = \begin{pmatrix} \Omega & V_1(p_{p+})^2 & 0 & V_2 p_{p+} p_{p-} \\ V_1(p^*_{p+})^2 & \Omega^* & V_2 p^*_{p+} p^*_{p-} & 0 \\ 0 & V_2 p_{p+} p_{p-} & \Omega & V_1(p_{p-})^2 \\ V_2 p^*_{p+} p^*_{p-} & 0 & V_1(p^*_{p-})^2 & \Omega^* \end{pmatrix} \tag{3}$$

Here we use $\Omega = (\omega_0 + \delta\omega_0 - \omega) - i\gamma$, where ω_0 is the bare frequency of the signal and idler modes, $\delta\omega_0$ takes into account possible blueshifts of the resonance condition, γ is the signal and idler inverse lifetime and ω is the laser frequency. So $(\omega_0 + \delta\omega_0 - \omega)$ corresponds to the detuning between the laser and the polaritonic modes.

We study the behaviour of the total idler intensity $I_i = |p_{i+}|^2 + |p_{i-}|^2$ by inverting M, using a source vector S describing a vertically polarised probe : $S = (1, 0, 1, 0)$ and a pump linearly polarised with an angle θ_p : $p_{p+} = e^{i\theta_p}$, $p_{p-} = e^{-i\theta_p}$. We assume that the resonance condition is met: $\Omega = -i\gamma$. Solving this system for pump powers far below the oscillation threshold, we obtain an expression of the idler intensity I_i that shows how it depends on the pump intensity I_p, signal (i.e. probe) intensity I_s, on the pump-probe angle θ_p, on the interaction potential V_1 and on the ratio V_2/V_1:

$$I_i \propto I_s I_p^2 V_1^2 \left(1 + \left(\frac{V_2}{V_1} \right)^2 + 2 \frac{V_2}{V_1} \cos(2\theta_p) \right) \tag{4}$$

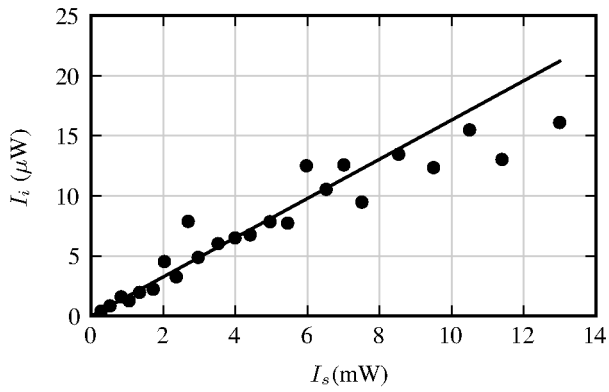

FIG. 6. Idler power I_i plotted against the probe power I_s. The dots are experimental data points, the solid curve is a linear fit to the low power data. See the text for the value of the fixed parameters.

IV. POWER BEHAVIOUR

We now study the experimental dependence of the idler intensity with respect to the excitation parameters. First, the idler intensity dependence on the probe power is shown in Fig. 6. The other parameters are fixed: the detuning $\delta = E_{\rm laser} - E_{\rm exciton}$ is -2.5 meV, the pump power is 50 mW and the pump and the probe beams are cross-polarised. The Eq. 4 anticipates a linear dependence for that measurement: $I_i \propto I_s$. This is what we observe up to a probe power of 8 mW. At higher probe powers, the idler intensity saturates. This indicates that the process efficiency is limited: an additional stimulation above 10 mW does not increase the scattering rate. Competing processes can explain this saturation, including mode shifts, pump depletion and crossed two-photon absorption of the probe with pump polaritons.[31]

Second, the idler intensity dependence on the pump power is shown in Fig. 7. In this set of data, the probe power is 2 mW, the detuning $\delta = E_{\rm laser} - E_{\rm exciton}$ is -2.8 meV, and the pump and the probe beams are cross-polarised. The Eq. 4 anticipates a quadratic dependance for that measurement: $I_i \propto I_p^2$. The data is correctly fitted with a square power law up to a pump power of 70 mW. For a pump power above 80 mW, the idler intensity decreases dramatically, showing that the parametric process stops. This is due to non-linear effects induced by the pump on the modes of the structure: the polariton branches widen and shift, the weak-coupling regime

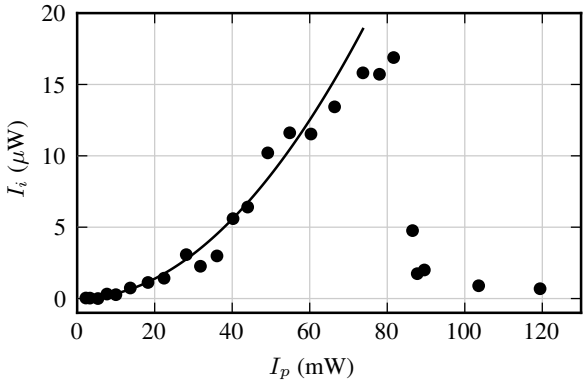

FIG. 7. Idler intensity I_i plotted against the pump power I_p. The dots are experimental data points, the solid curve is a square-law fit to the low-power data.

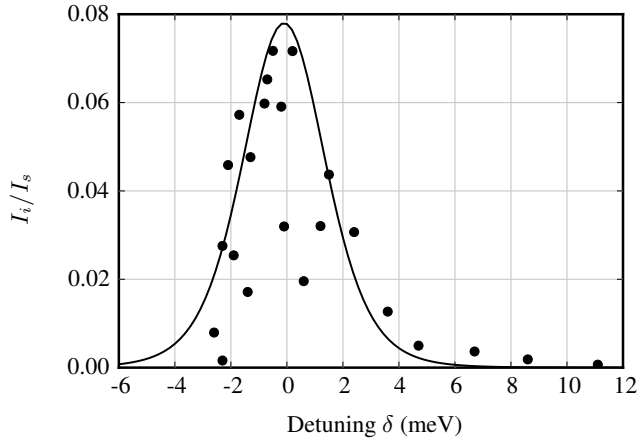

FIG. 8. Idler intensity I_i normalized by the probe intensity I_s and plotted against the laser detuning $\delta = E_p - E_X$. The solid curve is a fit with $X(\delta)^8$.

is approached, and consequently the probe beam is no longer in resonance and cannot enter the structure.

Third, the idler intensity dependence on the detuning $\delta = E_{\text{laser}} - E_{\text{exciton}}$ is shown in Fig. 8. Here, the pump power is fixed at 60 mW. The probe power is 2 mW. The probe and pump beams are cross-polarised. The enveloppe of this curve is bell-shaped with a maximum around zero detuning. For detunings lower than -3 meV, the idler was not visible. Variations below the enveloppe of Fig. 8 are attributed to situations where the spot superposition or the angles of incidence were sub-optimal. We observed that the process works at detunings which are close to zero in a weak-coupling configuration, where the beams can enter the sample through the cavity modes only weakly-coupled to the excitons. Still, the excitonic nonlinearity allows the parametric process to occur efficiently.

In the Eq. 4, the terms that directly depend[32] on the detuning δ are V_1 and V_2. The experimental setup corresponds to $\theta_p = \pi/2$, which gives $I_i \propto (V_1 - V_2)^2$. Now, each of these potentials depends on the detuning δ through the Hopfield coefficient[33] for the excitonic part of the polaritons: $V_i \propto X(\delta)^4$. This gives:

$$I_i \propto X(\delta)^8 = \left(\frac{\hbar\Omega}{\sqrt{(\hbar\Omega)^2 + 4(E - E_X)^2}} \right)^8 \qquad (5)$$

On Fig. 8, the fit with $X(\delta)^8$ correctly reproduces the envelope of the data points.

All these observations validate our theoretical description of the scattering process.

V. POLARISATION BEHAVIOUR AND V_2/V_1 MEASUREMENTS

Now that it is clear that the process that we observe is parametric and that the Eq. 4 satisfyingly describes the power dependences, we focus on the polarisation behaviour that will lead to measurements of the ratio V_2/V_1.

The fact that two polarisation-dependent scattering channels are present induces a rotation effect on the polarisation of the idler. At least at the lowest order in I_p, the interaction model anticipates that the idler is the symmetric of the signal with respect to the pump. This translates on the linear polarisation angles as:

$$\theta_i - \theta_p = \theta_p - \theta_s \qquad (6)$$
$$\Leftrightarrow \quad \theta_i = 2\theta_p - \theta_s \qquad (7)$$

The Fig. 9 presents a serie of measurements of the idler polarisation angle when the pump polarisation is rotated. The pump power is 60 mW, the probe power is 4 mW, and the laser-exciton detuning is -2.6 meV. The data shows that the idler angle θ_i varies with $2\theta_p - \theta_s$.

Now, looking at Eq. 4, it is clear that measuring how I_i depends on θ_p should provide enough data to estimate V_2/V_1, since $I_i \propto 1 + (V_2/V_1)^2 + 2(V_2/V_1)\cos(2\theta_p)$. The Fig. 10 shows one serie of raw measurements of I_i as a function of θ_p. The pump power is 60 mW, the probe power is 4 mW and the laser-exciton detuning is -2.6 meV. Although we see an obvious dependence on θ_p, the period of this dependence is twice as small as the one of $\cos(2\theta_p)$. We see two local maxima for parallel and perpendicular polarisations and a minimum around 40 degrees. This pronounced minimum at 40 degrees comes from the polarisation response of our visualisation setup, where the beams reach the CCD sensor used for intensity measurements by first going through various waveplates and being reflected on the spectrometer grating. This grating and the waveplates are sensible to the angle of linear polarisation of the idler. The waveplates also introduce a small elliptical component to the idler polarisation. The effective transfer function for these effects can be described with three separately-calibrated parameters: first, the ratio of the setup response with a

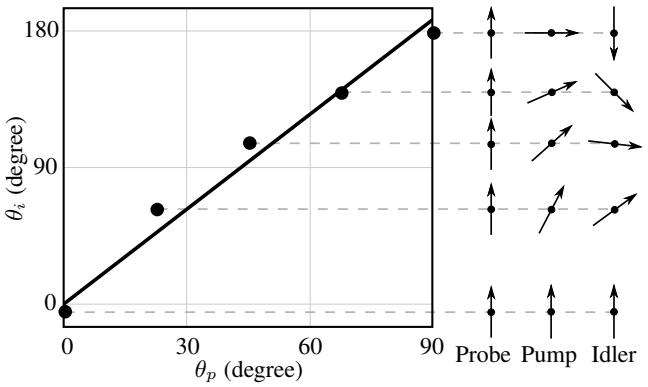

FIG. 9. Linear polarisation angle θ_i of the idler as a function of the linear polarisation angle of the pump θ_p. The linear polarisation of the probe is kept vertical while the pump angle is rotated from 0 degree (parallel to the probe) to 90 degrees (perpendicular). The dots are the experimental data points. The solid line is a fit with $\theta_i = 2\theta_p - \theta_s$.

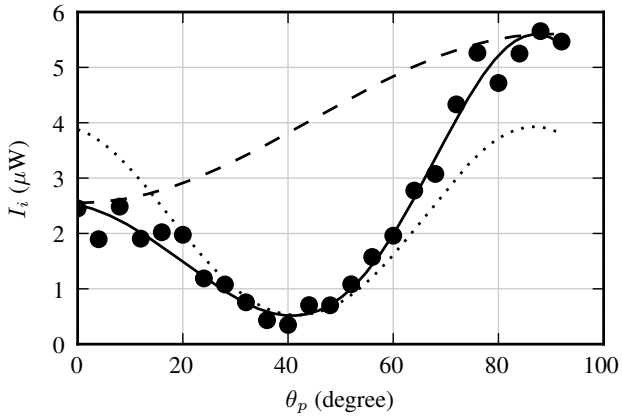

FIG. 10. Idler intensity I_i plotted against the relative polarisation θ_p of the pump and the probe. The dots are the raw experimental data. The probe polarisation is fixed vertically, while the pump polarisation is rotated incrementally between 0 degree (parallel) and 90 degrees (orthogonal). The solid curve is a fit including the polarisation response of the visualization setup and the existence of the two polarisation channels. The dashed curve illustrates the same fit for a flat polarisation response. The dotted curve illustrates the same fit when neglecting V_2, i.e. when ignoring the scattering channel that inverses circular polarisation.

horizontal polarisation with respect to a vertical polarisation $\rho = horizontal/vertical = 0.068$; second, a constant angle shift θ_0 = -3.2 degrees which corresponds to the difference between the vertical as measured by the reference polariser and as defined by the slit and the grating of the spectrometer; third, an elliptical component represented by an angle $\psi = 15$ degrees. The polarisation response of the setup brings an additional multiplicative term $f(\theta_i)$ in the expression of I_i:

$$\begin{aligned} f(\theta_i) \propto & \cos^2\left(\psi \sin(2(\theta_i-\theta_0))\right)\cos^2\left(2(\theta_i-\theta_0)\right) \\ & + \sin^2\left(\psi \sin(2(\theta_i-\theta_0))\right)\sin^2\left(2(\theta_i-\theta_0)\right) \\ & + \rho\cos^2\left(\psi \sin(2(\theta_i-\theta_0))\right)\cos^2\left(2(\theta_i-\theta_0)-\frac{\pi}{2}\right) \\ & + \rho\sin^2\left(\psi \sin(2(\theta_i-\theta_0))\right)\sin^2\left(2(\theta_i-\theta_0)-\frac{\pi}{2}\right) \end{aligned} \tag{8}$$

The shape of $f(\theta_i)$ correctly describes the minimum at 40 degrees. Now the assymetry between 0 and 90 degrees is not explained at all by the polarisation response of the setup but by the Eq. 4 when V_2 is non-zero. We finally fit the experimental points in Fig. 10 with:

$$a f(\theta_i)\left(1+\left(\frac{V_2}{V_1}\right)^2 + 2\frac{V_2}{V_1}\cos(2\theta_p)\right) \tag{9}$$

where a is a multiplicative constant. The fit leads us to a relative measure of V_2 for this particular detuning:

$$V_2 \approx -0.19 V_1 \tag{10}$$

Alternatively we show on Fig. 11 the experimental measurements normalised by the setup response $f(\theta_i)$ to better highlight the variation that solely comes from the parametric interaction model. The fit is directly done with $I_i \propto 1 + (V_2/V_1)^2 + 2(V_2/V_1)\cos(2\theta_p)$, so that the unique adjustable parameter is V_2/V_1.

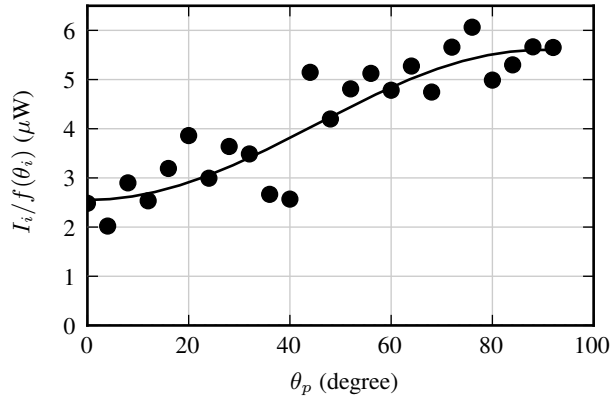

FIG. 11. Idler intensity I_i normalized over the polarisation response $f(\theta_i)$ of the visualization setup and plotted as a function of the relative polarisation θ_p of the pump and the probe. The dots are the experimental data. The probe polarisation is fixed vertically, while the pump polarisation is rotated incrementally between 0 degree (parallel) and 90 degrees (orthogonal).The solid curve is a fit including the effect of the two polarisation-dependent scattering channels.

VI. V_2/V_1 AS A FUNCTION OF THE DETUNING

Since the value of V_2/V_1 has been shown to depend on the detuning in previous studies[9], we now use our setup to measure that value over a range of detunings that have not been explored up to now. We conducted this study over a range of laser-exciton detunings going from -2 meV to +5 meV. The results are reproduced in Fig. 12. We

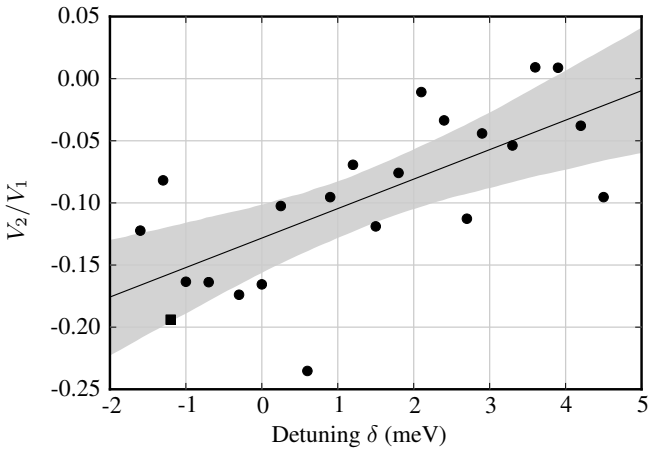

FIG. 12. Ratio V_2/V_1 of the polarisation-dependent scattering strengths measured over a range of laser-exciton detunings $\delta = E_p - E_X$. The square data point corresponds to the measurements presented in Fig. 10. The solid line is a linear regression. The shaded area is a 95% confidence region for this linear regression, bounded by the 2.5% and 97.5% quantiles.

find that V_2/V_1 increases progressively from -0.2 to 0 on this range of detunings.

This range of values is in good agreement with the previous estimation in Ref. 34, which gives $V_2 \approx -0.04V_1$ in a single MC with one QW for a fixed cavity-exciton detuning of 0 meV, which approximately corresponds to a laser-exciton detuning δ of -2 meV in our sample. Ref. 16 gives $V_2 \approx -0.08V_1$ for a fixed cavity-exciton detuning of 0 meV, which is in even better agreement with our measurements.

In the range of detunings studied here, our measurements show that the ratio V_2/V_1 is increasing with the detuning. Assuming that the dependency of the ratio V_2/V_1 as a function of detuning is linear in this range, we have run a regression analysis on the measurements, finding an average increase from -0.175 to -0.01. Performing a Monte-Carlo Bayesian inference regression[35,36], we compute the probability distribution for the parameters of the fit to quantify how confident we can be in the increase of the ratio V_2/V_1. The shaded area in Fig. 12 represents the 95% confidence region for the regression, bounded by the 2.5 % and 97.5 % quantiles obtained by the Bayesian method. This statistically confirms that the interaction ratio is actually increasing with the detuning.

The measurements in this paper shall now be compared to those obtained in Ref. 9. This work indicates that V_2/V_1 decreases progressively from 0 to -1 for cavity-exciton detunings going from -3.0 meV to 0.0 meV. Given the Rabi splitting of 3.5 meV in their sample, this range of cavity-exciton detunings corresponds to laser-exciton detunings δ going from -4.0 to -1.2 meV. For larger detunings, the measurements of Ref. 9 are highly dispersed and no tendency stands out. In contrast, our method provides data for detunings δ above -1.5 meV and up to 4.5 meV and indicates that V_2/V_1 increases progressively from -0.2 to 0.0. Our study confirms the major result of Ref. 9: the ratio V_2/V_1 is not a constant. We note three differences in the results of the two studies : we have studied a different range of detunings, we see a lower amplitude of variation of the ratio V_2/V_1 (0.2 meV versus 1 meV), and we see this ratio increasing with detuning whereas it was found to be decreasing in Ref. 9. It is worth noting that these two studies are done in very different conditions. Not only the accessible detuning range is different, but there are also differences in the sample structure: we study a multiple MC instead of a single MC and our structure contains six QWs instead of one. These choices provide us more flexibility and more efficiency in the nonlinear processes. It is also worth noting that we study the sample using a resonant continuous incident light source instead of a pulsed source with a wide spectrum. The single-vs-multiple QWs situation is the main candidate for the difference in behaviour. We conclude this comparison by emphasizing that the method we used is experimentally convenient and provides straightforward measurements of V_2/V_1 over a wide range of parameters.

The values of V_2/V_1 measured in this work have interesting consequences. We mention here what these consequences are in the context of parametric oscillation. In the parametric scattering process which can lead to parametric oscillation, the gain is proportional to $V_1 + V_2$ when the linear polarisation is conserved, and to $V_1 - V_2$ when the linear polarisation is reversed. Since we have measured that V_2/V_1 is negative and its absolute value is smaller than 1 in the range of detunings studied, it is in the configuration that reverses the linear polarisation that the parametric oscillation is expected to happen. This corresponds well to experimental observations[3,37,38]. This polarisation selectivity is all the more pronounced when the pump energy is well below the excitonic transition. On the other hand, if we extrapolate the data points for laser-exciton detuning above 5 meV, we can expect V_2 to become positive. It means that for these large detunings the regime of parametric oscillation would be expected to change dramatically and the process would conserve the linear polarisation.

CONCLUSION

We have reported the study of the polarisation-dependent polariton-polariton interaction potentials in a triple-MC by observing the energy-degenerate stimulated parametric scattering of polaritons. In this process, a probe beam stimulates the scattering of two pump polaritons into a signal and an idler polaritons of the same energy, conserving energy and momentum. The idler behaviour follows an interaction model that takes into account two polarisation-dependent scattering channels. This has allowed us to measure the relative value of the anti-circular interaction potential V_2 compared to its co-circular counterpart V_1 with a convenient and pre-

cise method. We analysed this ratio over a large range of detuning and found it to be highly detuning-dependant: it goes from -0.2 to 0 for laser-exciton detunings going from -2 meV to +5 meV. This study complements earlier results[9] in a range of detunings unexplored to-date. This shows the flexibility of a multiple MC, and we believe these results are precious for the study of spin-dependent nonlinear phenomena in MCs.

[a] Email address: lecomte.timothee@gmail.com; Present Affiliation: Institut Pasteur, Unité d'Analyse d'Images Biologiques, CNRS URA 2582, 75015 Paris, France
[b] Present Affiliation: ETH Zurich, Institut f. Polymere, 8093 Zurich, Switzerland

[1] P. G. Savvidis, J. J. Baumberg, R. M. Stevenson, M. S. Skolnick, D. M. Whittaker, and J. S. Roberts, Physical Review Letters **84**, 1547 (2000).
[2] J. J. Baumberg, P. G. Savvidis, R. M. Stevenson, A. I. Tartakovskii, M. S. Skolnick, D. M. Whittaker, and J. S. Roberts, Physical Review B **62**, R16247 (2000).
[3] C. Diederichs, J. Tignon, G. Dasbach, C. Ciuti, A. Lemaître, J. Bloch, P. Roussignol, and C. Delalande, Nature **440**, 904 (2006).
[4] J. Kasprzak, M. Richard, S. Kundermann, A. Baas, P. Jeambrun, J. M. J. Keeling, F. M. Marchetti, M. H. Szymanska, R. Andre, J. L. Staehli, V. Savona, P. B. Littlewood, B. Deveaud, and L. S. Dang, Nature **443**, 409 (2006).
[5] K. G. Lagoudakis, M. Wouters, M. Richard, A. Baas, I. Carusotto, R. Andre, L. S. Dang, and B. Deveaud-Pledran, Nat Phys **4**, 706 (2008).
[6] A. Amo, J. Lefrère, S. Pigeon, C. Adrados, C. Ciuti, I. Carusotto, R. Houdré, E. Giacobino, and A. Bramati, Nature Physics **5**, 805 (2009).
[7] R. Hivet, H. Flayac, D. Solnyshkov, D. Tanese, T. Boulier, D. Andreoli, E. Giacobino, J. Bloch, A. Bramati, G. Malpuech, and A. Amo, Nature Physics **8**, 724 (2012).
[8] I. A. Shelykh, A. V. Kavokin, Y. G. Rubo, T. C. H. Liew, and G. Malpuech, Semiconductor Science and Technology **25**, 013001 (2010).
[9] M. Vladimirova, S. Cronenberger, D. Scalbert, K. V. Kavokin, A. Miard, A. Lemaître, J. Bloch, D. Solnyshkov, G. Malpuech, and A. V. Kavokin, Physical Review B **82**, 075301 (2010).
[10] C. Adrados, A. Amo, T. C. H. Liew, R. Hivet, R. Houdré, E. Giacobino, A. V. Kavokin, and A. Bramati, Physical review letters **105**, 216403 (2010).
[11] D. Sarkar, S. S. Gavrilov, M. Sich, J. H. Quilter, R. A. Bradley, N. A. Gippius, K. Guda, V. D. Kulakovskii, M. S. Skolnick, and D. N. Krizhanovskii, Physical Review Letters **105**, 216402 (2010).
[12] A. Amo, T. Liew, C. Adrados, R. Houdré, E. Giacobino, A. Kavokin, and A. Bramati, Nature Photonics **4**, 361 (2010).
[13] G. Dasbach, T. Baars, M. Bayer, A. Larionov, and A. Forchel, Physical Review B **62**, 13076 (2000).
[14] P. G. Lagoudakis, P. G. Savvidis, J. J. Baumberg, D. M. Whittaker, P. R. Eastham, M. S. Skolnick, and J. S. Roberts, Physical Review B **65**, 161310 (2002).
[15] P. Renucci, T. Amand, X. Marie, P. Senellart, J. Bloch, B. Sermage, and K. V. Kavokin, Physical Review B **72**, 075317 (2005).
[16] D. D. Solnyshkov, I. A. Shelykh, M. M. Glazov, G. Malpuech, T. Amand, P. Renucci, X. Marie, and A. V. Kavokin, Semiconductors **41**, 1080 (2007).
[17] D. N. Krizhanovskii, D. Sanvitto, I. A. Shelykh, M. M. Glazov, G. Malpuech, D. D. Solnyshkov, A. Kavokin, S. Ceccarelli, M. S. Skolnick, and J. S. Roberts, Physical Review B **73**, 073303 (2006).
[18] J. Kasprzak, R. André, L. S. Dang, I. A. Shelykh, A. V. Kavokin, Y. G. Rubo, K. V. Kavokin, and G. Malpuech, Physical Review B **75**, 045326 (2007).
[19] Z. Vörös, D. W. Snoke, L. Pfeiffer, and K. West, Physical Review Letters **103**, 016403 (2009).
[20] A. I. Bobrysheva, M. F. Miglei, and M. I. Shmiglyuk, Physica Status Solidi (b) **53**, 71 (1972).
[21] C. Ciuti, V. Savona, C. Piermarocchi, A. Quattropani, and P. Schwendimann, Physical Review B **58**, 7926 (1998).
[22] M. Combescot, O. Betbeder-Matibet, and R. Combescot, Physical Review Letters **99**, 176403 (2007).
[23] S. Schumacher, N. H. Kwong, and R. Binder, Physical Review B **76**, 245324 (2007).
[24] M. Wouters, Physical Review B **76**, 045319 (2007).
[25] M. M. Glazov, H. Ouerdane, L. Pilozzi, G. Malpuech, A. V. Kavokin, and A. D'Andrea, Physical Review B **80**, 155306 (2009).
[26] M. Saba, C. Ciuti, J. Bloch, V. Thierry-Mieg, R. Andre, L. S. Dang, S. Kundermann, A. Mura, G. Bongiovanni, J. L. Staehli, and B. Deveaud, Nature **414**, 731 (2001).
[27] C. Ciuti, P. Schwendimann, B. Deveaud, and A. Quattropani, Physical Review B **62**, R4825 (2000).
[28] C. Diederichs and J. Tignon, Applied Physics Letters **87**, 251107 (2005).
[29] D. Taj, T. Lecomte, C. Diederichs, P. Roussignol, C. Delalande, and J. Tignon, Physical Review B (Condensed Matter and Materials Physics) **80**, 081308 (2009).
[30] C. Ciuti, P. Schwendimann, and A. Quattropani, Semiconductor Science and Technology **18**, S279 (2003).
[31] Y. R. Shen, *The Principles of Nonlinear Optics* (Wiley-Interscience, 2002).
[32] It is worth noting that the experiment is performed for constant incident *intensities* and not for constant *populations*. The model predicts the evolution of populations, and the relation between the intracavity populations and the incident intensities also depends on the detuning. Nevertheless, as shown later, taking into account the variations of V_1 and V_2 only is enough to reproduce the enveloppe of the experimental data with a satisfying precision.
[33] J. J. Hopfield, Physical Review **112**, 1555 (1958).
[34] K. Kavokin, P. Renucci, T. Amand, X. Marie, P. Senellart, J. Bloch, and B. Sermage, physica status solidi (c) **2**, 763 (2005).
[35] A. Gelman, J. Carlin, H. Stern, and D. Rubin, *Bayesian Data Analysis, Second Edition*, Chapman & Hall/CRC Texts in Statistical Science (Taylor & Francis, 2003).
[36] Stan Development Team, *Stan: A C++ Library for Probability and Sampling, Version 2.1* (http://mc-stan.org/, 2013).

[37] G. Dasbach, C. Diederichs, J. Tignon, C. Ciuti, P. Roussignol, C. Delalande, M. Bayer, and A. Forchel, Physical Review B **71**, 161308 (2005).

[38] M. Romanelli, C. Leyder, J. P. Karr, E. Giacobino, and A. Bramati, Physical Review Letters **98**, 106401 (2007).